

Figure 2. The cross section,  $D_\lambda$  and  $D_\sigma$  angular distributions for the isoscalar transitions in  $^{10}\text{B}(\vec{p}, \vec{p}')^{10}\text{B}$ . The curves represent the effective interaction of Seifert, *et al.*

MEASUREMENT OF THE REMAINING IN-PLANE POLARIZATION TRANSFER  
COEFFICIENTS FOR THE  $^{10}\text{B}(\vec{p}, \vec{p}')^{10}\text{B}$  REACTION AT 200 MeV

A.C. Betker, A.D. Bacher, W.A. Franklin, D.L. Prout,  
E.J. Stephenson, S.W. Wissink, and C. Yu  
*Indiana University Cyclotron Facility, Bloomington, Indiana, 47408*

H. Baghaei and R.A. Lindgren  
*University of Virginia, Charlottesville, Virginia 22901*

J.A. Carr and F. Petrovich  
*Florida State University, Tallahassee, Florida 32206*

In order to understand the modification of the nucleon-nucleon force within the nuclear medium, we have undertaken the measurement of several "stretched states" that have well understood structure. In the case of  $^{10}\text{B}$  the state of interest is the the  $0^+$  state at 1.74 MeV. This transition has a single-particle, single-hole configuration with a well

determined magnetic form-factor from electron scattering studies,<sup>1</sup> is an isospin  $\Delta T=1$  transition, and because of its low excitation energy, is cleanly accessible to large momentum transfer. Previous experiments<sup>2,3</sup> have measured cross-section  $d\sigma/d\Omega$ , analyzing power  $A$ , induced polarization  $P$ , normal component spin transfer  $D_{NN}$  and two combinations of the four in-plane spin transfer coefficients, denoted as  $D_\sigma$  and  $D_\lambda$ . These experiments have been performed with the K600 spectrometer and have utilized its high resolution properties to separate the state of interest from other nearby states.

Parity conservation permits polarimeters to measure only the in-plane projection of the scattered proton polarization that is sideways at the polarimeter's carbon analyzer target. Precession in the K600 spectrometer's magnetic field yields two linear combinations,  $D_\sigma$  and  $D_\lambda$ , of the four in-plane polarization transfer coefficients as the observables associated with sideways and longitudinal beam polarization. They are given by

$$D_\sigma = D_{SS'} \cos \alpha + D_{SL'} \sin \alpha, \quad \text{and}$$

$$D_\lambda = D_{LS'} \cos \alpha + D_{LL'} \sin \alpha$$

where  $\alpha$  is the spin precession angle through the K600. For the previous data set  $\alpha = 235^\circ$ . This experiment utilized the new "super-low" dispersion mode of the K600, described elsewhere in this report,<sup>4</sup> to repeat the in-plane spin transfer measurements with  $\alpha \simeq 300^\circ$ . Once these data are analyzed, this will allow us to extract all four of the standard in-plane spin transfer coefficients.

These new measurements were performed at  $\theta_{lab}=20^\circ, 31^\circ, 40^\circ, 48^\circ,$  and  $60^\circ$ , the same angles at which the other in-plane data were taken. The best resolution achieved was 40 keV FWHM, although most of the data was taken with thick targets to maximize data rate. Resolution was most critical at  $31^\circ$  and  $48^\circ$ , where the state of interest is close to contaminant states from  $^{11}\text{B}$  and  $^{12}\text{C}$  in the target. A resolution of 150-200 keV, which was typical, was sufficient for this purpose.

The data were taken with three different settings of the spin precession solenoids in the high energy beam lines. While two settings are sufficient to obtain longitudinal and sideways measurements, using three settings, spaced about  $60^\circ$  apart, gave a simultaneous systematic evaluation of the system. At all five scattering angles, the measured asymmetry was well reproduced by a sinusoidal function of the in-plane spin direction.

The previous data are shown in Fig. 1. The curves are from DW81 calculations<sup>5</sup> with different  $t$ -matrices to describe the interaction. The  $t$ -matrix was parameterized with three terms:

$$t(\rho) = t_{FREE} + \Delta t_{MOD} \cdot \rho + \Delta t_{PAULI}(\rho)$$

where  $\rho$  is the local nuclear density. This was motivated by QCD sum rule calculations which suggest that the density-dependence that arises from nucleon and meson substructure varies linearly with density over the range sampled by our experiment.<sup>6</sup> Since we wish to characterize this piece of the density-dependence using our data, a phenomenological term,  $\Delta t_{MOD} \cdot \rho$ , has been included. The  $t_{FREE}$  term is similar to the Franey-Love  $t$ -matrix,<sup>7</sup> but is derived directly from the SM93 nucleon-nucleon phase shift solution at 200 MeV by Arndt,<sup>8</sup> and as such is better constrained because it is based on significantly more, higher precision data. The  $\Delta t_{PAULI}(\rho)$  term is the *change* in the  $t$ -matrix due to

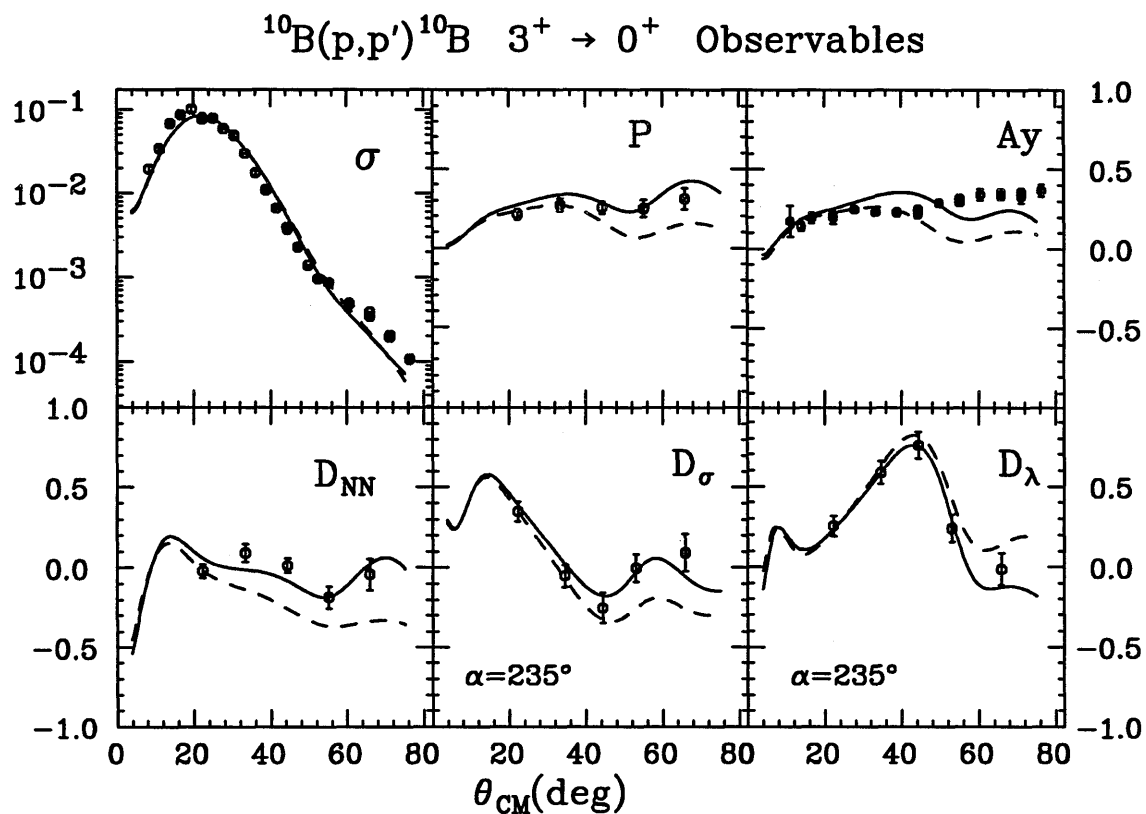


Figure 1. Previously measured  $^{10}\text{B} \ 3^+ \rightarrow 0^+$  observables, along with DWBA calculations. The dashed lines represent a  $t$ -matrix composed of  $t_{\text{FREE}} + \Delta t_{\text{PAULI}}(\rho)$ . The solid curves include an additional phenomenological term,  $\Delta t_{\text{MOD}} \cdot \rho$ .

binding energy and Pauli blocking in the medium as calculated by Nakayama and Love.<sup>9</sup> In Fig. 1, the dashed curve includes the SM93  $t$ -matrix and the Pauli term, while the solid curve includes all three terms. The phenomenological term, parameterized as density-changes to the  $J \leq 2$  nucleon-nucleon phase-shifts of SM93, was adjusted to best reproduce the data in Fig. 1.

As a test of the quality of the phenomenological adjustment, predictions, shown in Fig. 2, were made for the new measurements. On-line data points from an experiment completed in March, 1995 are included. After a complete analysis, statistical precision is expected to improve slightly, and any systematic effects will be included.

It appears that the phenomenological modification that was appropriate for the previous data is worse than no modification for the new data. Thus the new measurements contain constraints that were not present in the old analysis, and they will clearly be useful in specifying the character of the in-medium interaction. A full set of polarization-transfer coefficients will now allow the separation of the data into pieces that are sensitive to individual KMT amplitudes and the individual transverse and spin-longitudinal responses of the nucleus.<sup>10</sup> Future studies of the in-medium effects will be pursued along these lines.

$^{10}\text{B}(p,p')$   $E_p=200\text{MeV}$   $\alpha=305^\circ$

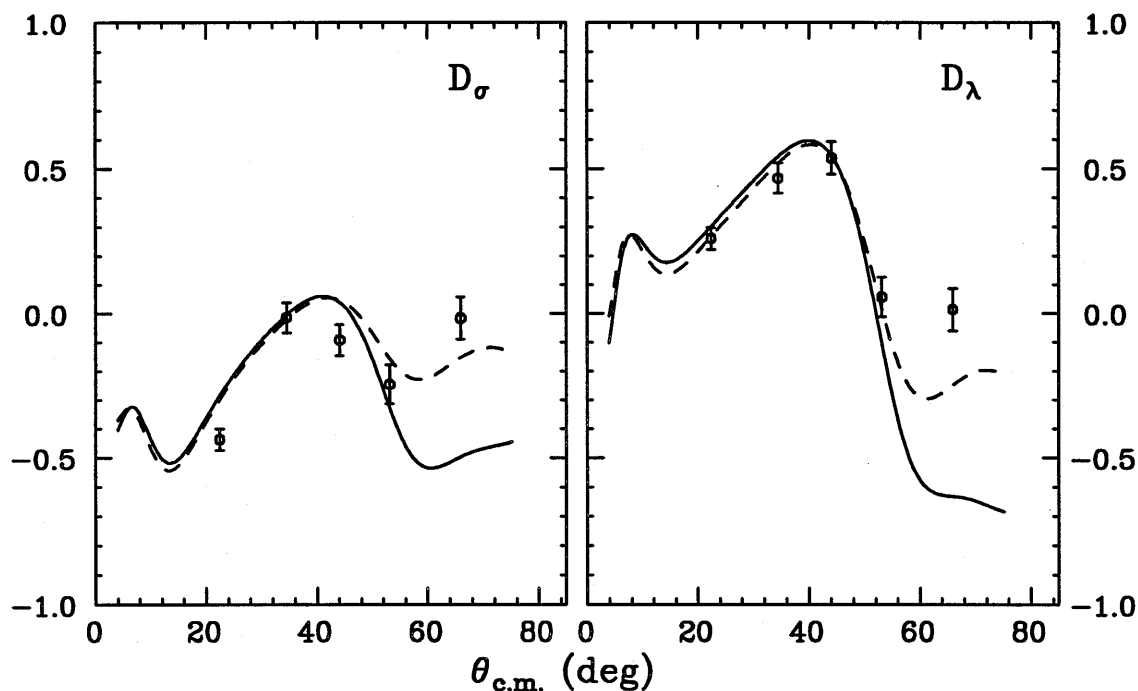


Figure 2. Predictions for  $D_\sigma$  and  $D_\lambda$  at  $\alpha = 305^\circ$ , along with the new data points. The curves are described in Fig. 1.

1. R.S. Hicks, *et al.*, Phys. Rev. Lett. **60**, 905 (1988).
2. H. Baghaei, *et al.*, Phys. Rev. C **69**, 2054 (1992).
3. S. Chang, *et al.*, IUCF Sci. and Tech. Rep., May 1992 - April 1993, p. 16.
4. A.D. Bacher, *et al.*, this report.
5. R. Schaeffer and J. Raynal, program DW81, private communication.
6. For example, T. Hatsuda and S. Huong Lee, Phys. Rev. C **43**, 213 (1991); M. Asakawa and C.M. Ko, Phys. Rev. C **48**, R526 (1993).
7. M.A. Franey and W.G. Love, Phys. Rev. C **31**, 488 (1985).
8. R. Arndt, private communication.
9. K. Nakayama and W.G. Love, Phys. Rev. C **38**, 51 (1988).
10. E. Bleszynski, M. Bleszynski, and C.A. Whitten, Jr., Phys. Rev. C **26**, 2063 (1982); J.M. Moss, Phys. Rev. C **26**, 727 (1982).